Editors' Suggestion

Evaporative cooling from an optical dipole trap in microgravity

Christian Vogt, Marian Woltmann, Sven Herrmann, and Claus Lämmerzahl
ZARM, University of Bremen, Am Fallturm, D-28359 Bremen, Germany

Henning Albers, Dennis Schlippert, and Ernst M. Rasel
Institute of Quantum Optics and QUEST-Leibniz Research School, Leibniz Universität Hannover, Welfengarten 1, D-30167 Hannover, Germany

(PRIMUS)

(Received 24 September 2019; published 28 January 2020)

In recent years, cold atoms could prove their scientific impact not only on ground but in microgravity environments such as the drop tower in Bremen, sounding rockets, and parabolic flights. We investigate the preparation of cold atoms in an optical dipole trap, with an emphasis on evaporative cooling under microgravity. Up to 1×10^6 rubidium-87 atoms were optically trapped from a temporarily dark magneto-optical trap during free fall in the drop tower in Bremen. The efficiency of evaporation is determined to be equal with and without the effect of gravity. This is confirmed using numerical simulations that prove the dimension of evaporation to be three dimensional in both cases due to the anharmonicity of optical potentials. These findings pave the way towards various experiments on ultracold atoms under microgravity and support other existing experiments based on atom chips but with plans for additional optical dipole traps such as the upcoming follow-up missions to past and current space-borne experiments.

DOI: 10.1103/PhysRevA.101.013634

I. INTRODUCTION

Atom interferometry is a precise quantum tool that will enhance a broad variety of measurements, ranging from large scale phenomena like gravitational wave detection [1–3] to short scale Casimir-Polder forces and many things in between [4]. Its sensitivity largely benefits from long evolution times between laser pulses [5] as provided by levitation [6] or operation in microgravity [7–11]. The latter can only be realized with ultracold atomic ensembles because of their low expansion rates. The preparation of ultracold atoms generally follows the same path. Atoms are laser cooled in a magneto-optical trap (MOT) before they are transferred into a purely optical or magnetic potential, where they are further cooled by evaporative cooling. In this relatively slow process the temperature is decreased at the cost of atom losses. Even though the creation of Bose-Einstein condensates (BECs) could be demonstrated by laser cooling mechanisms lately [12–14], the lowest expansion rates realized [15,16] are based on evaporative cooling [17] and delta-kick collimation [18]. The former can either be implemented by the rf-knife method in magnetic traps or by lowering the optical potential confining an atomic ensemble. In spite of optical traps being a commonly used tool in cold atom experiments to trap, cool, and manipulate atoms with low or vanishing magnetic susceptibility, to create quantum matter, to establish periodic crystals made out of light, and to exploit Feshbach resonances, evaporation therein has never been realized in microgravity before. Achievements such as the first BEC in space [9] or the realization of atom interferometry in microgravity [19] were based on magnetic traps, implemented on atom chips [20,21]. Thanks to the complementary advantages of dipole traps with respect to the manipulation with atom chips, we anticipate many applications for combining both approaches. In parallel with this work, Condon *et al.* [22] demonstrated a dipole trap on an Einstein elevator. While we focus on the dipole trap behavior in microgravity, they prioritize a long investigation time for the cold atomic ensemble in weightlessness. Therefore, the preparation of cold atoms is mainly executed before the microgravity phase. Our demonstration of the trapping and evaporative cooling process in weightlessness is an important stepping stone to realize this kind of experiment in future space missions [23,24].

II. EXPERIMENTAL SETUP

Our experimental setup (Fig. 2) has been described in detail before [25,26]. Here we give a short summary of the main components and the techniques used in this work. The whole apparatus is portable and can be run autonomously with no external supply connections. Since it is operated in the drop tower in Bremen, it fits into the standard drop tower capsule, which is 2 m high and has a diameter of 700 mm. The scientific payload is mounted on seven platforms with a total area of 2.5 m^2 attached to a cage formed by four aluminum stringers. Atoms are released from an oven, a heated copper tube with a rubidium reservoir. To prevent molten rubidium or glass particles from drifting into the vacuum chamber in microgravity, a bronze mesh is placed between the oven and vacuum chamber. Atoms are precooled in a $2D^+$MOT configuration [27] with two retroreflected beams and four magnetic coils in a racetrack configuration. The atoms are

	MOT	TDM I	TDM II	Hold	Evaporation	TOF	Image	Wait	Image
Time (ms)	1000	13	2	50	4 x 500	5-12.5	50	200	50
3D Cool Int. (mW)	20	20	20	0	0	0	20	0	20
3D Rep. Int. (mW)	3	3	0.03	0	0	0	3	0	3
3D Cool Det. (MHz)	14	120	120	-	-	-	10	-	10
3D Rep Det. (MHz)	0	0	0	-	-	-	0	-	0
B-Field (G/cm)	15	15	15	0	0	0	0	0	0
Dipole Power (W)	7	7	7	7	5.6 3.8 2.9 2.5	0	0	0	0

FIG. 1. Depicted is the experimental sequence for the applied evaporation. The MOT loading is followed by a temporarily dark MOT scheme; the evaporation is interrupted at four different times. Fluorescence images were taken after varying times of flight to determine the ensemble temperature. The camera's shutter opens for 600 μs per image.

optically pushed through a differential pumping tube into a three-dimensional (3D) MOT consisting of six individual laser beams, which are not exactly power balanced due to a fixed fiber splitter. Cooling and repumping light is generated by semiconductor laser diodes with the cooling laser in MOPA (master oscillator power amplifier) configuration. The dipole trap is formed by a thulium fiber laser, emitting at 1949 nm, with a maximum optical power of approximately 7 W at the atoms' position. The beam intensity is regulated by a Pockels cell and two Glan-laser polarizers. The collimated beam is focused by a single lens down to a waist of 45 μm into the center of the vacuum chamber. The vacuum quality of a few parts in 10^{-9} hPa is maintained by an ion getter and two chemical pumps. The entire setup is capable of withstanding drops in the 110 m drop tower with decelerations of up to 40 times Earth's gravitational acceleration. The available microgravity time is limited to 4.7 s per drop and can be used by our experiment twice a day. The performed experimental sequence is shown in Fig. 1 and allows for two data points per drop.

III. DIPOLE TRAP LOADING

The precooling phase starts with a 3D MOT which is fed by a 2D$^+$MOT. In this configuration approximately 1.5×10^9 atoms of rubidium-87 can be trapped within one and a half seconds, while the MOT performs almost equally in microgravity and on ground [Fig. 3(a)]. The recorded atom numbers are fitted to

$$N_{\mathrm{MOT}}(t) = \frac{R_{0_{\mathrm{MOT}}}}{\alpha}\left(1 - e^{(-\alpha t)}\right), \tag{1}$$

where $N_{\mathrm{MOT}}(t)$ is the number of atoms which are loaded into the MOT, $R_{0_{\mathrm{MOT}}}$ is the initial trap loading rate, α describes losses caused by collisions with residual background gas atoms, and t is the loading time. The initial loading rate is determined to be $R_{0_{\mathrm{MOT}}} = 1.3 \times 10^9$ atoms s^{-1} (1.4×10^9 atoms s^{-1}) for operation with (and without) gravity. The corresponding fits are displayed for a data set recorded under gravity (dashed orange) and in microgravity (solid blue) in Fig. 2. At this point, the atoms are about an order of magnitude too hot to be optically trapped in our system. Transferring them into the dipole trap needs further cooling. The most efficient loading was obtained by employing a temporarily dark MOT (TDM) scheme in which the repumper intensity is decreased, while the cooling light is detuned further to the red with respect to the cooling transition. In addition to the cooling effect, this method compresses the atomic ensemble and thereby increases the transition efficiency into the optical potential. In the current setup the cooling light detuning is

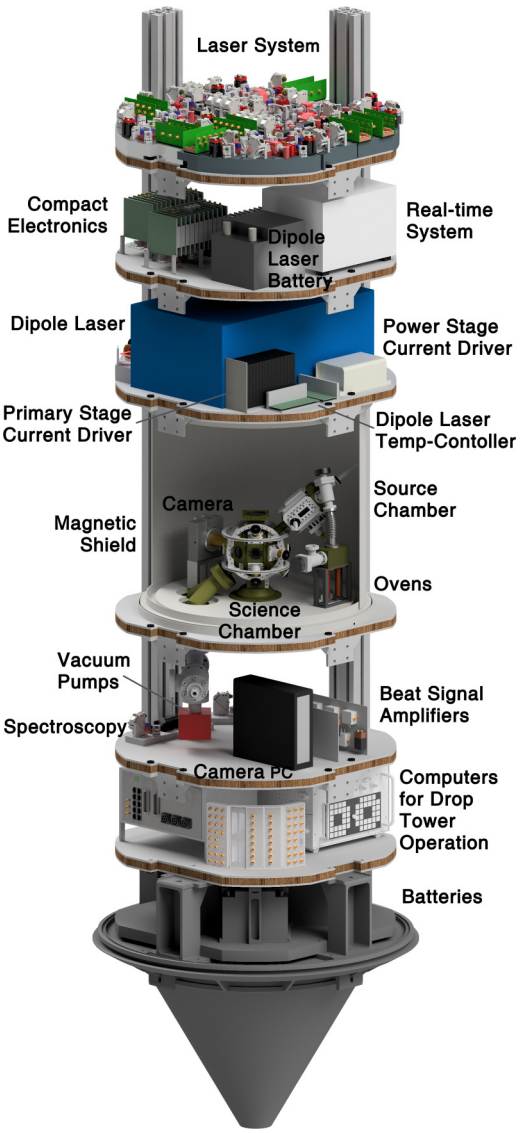

FIG. 2. CAD drawing of the entire autonomous and compact experimental setup. The device is approximately 2 m high with a diameter of 70 cm.

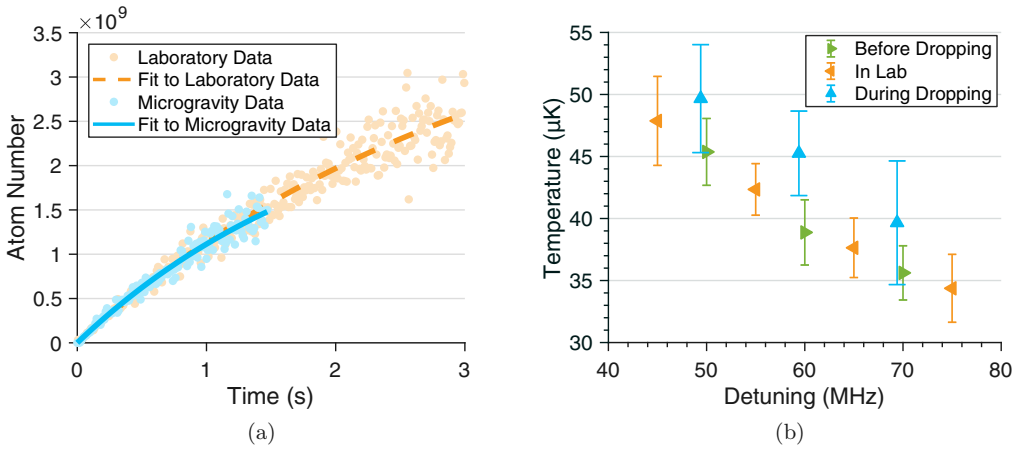

FIG. 3. (a) Loading dynamics for our three-dimensional MOT in microgravity and on ground. Approximately 1.5×10^9 are loaded within 1.5 s. The fluorescent signals for loading in gravity (orange dots) and under microgravity (blue dots) are plotted. Both data sets are fitted with Eq. (1) and the resulting curves are shown as solid blue for microgravity and dashed orange for gravity data. (b) Comparison of the TDM performance in the laboratory (orange), in the drop tower under gravity (green), and in microgravity (blue). In free fall the TDM efficiency is decreased leading to a temperature increase of a few μK. This is attributed to less stable laser frequency locks.

restricted to a maximum value of 120 MHz ($\approx$19.8 Γ) with respect to the $F = 2 \rightarrow F' = 3$ transition. Here Γ is the natural linewidth of the D_2 line of rubidium-87. In combination with a decreased rempumping beam power of 0.2 W m^{-2} this leads to a temperature of (28.0 ± 0.5) μK. In contrast to the MOT, the TDM performance is worsened in microgravity, as can be seen in Fig. 3(b). This is attributed to less stable frequency locks during the drop, caused by sudden mechanical and electrical changes when releasing the capsule. Nevertheless the performance was found to be sufficient to effectively load an optical dipole trap. Due to the choice of a dipole trapping laser with 1949 nm wavelength, we are able to load the dipole trap directly from the MOT [28], without an intermediate magnetic trapping or gray molasses scheme [29]. This is enabled by the same wavelength dependent sign of the complex polarizability for the ground and excited state of the MOT transition in rubidium-87 [30,31]. Optimal loading was observed with the laser parameters determined in the former section but timing was found to be crucial. By splitting the TDM scheme into two separate steps for detuning and intensity reduction with durations of 13 and 2 ms respectively, up to 5×10^6 atoms could be transferred into the optical trap. Furthermore, we can confirm a strong atom number dependency on the overlap between both traps [32]. Even though the free beam path of the dipole trapping laser spanning more than 1 m, including mirrors on different platforms, gave rise to pointing variations between drops, the recorded atom numbers showed no significant difference between ground based and drop tower operation. Figure 4 shows the fluorescence of atoms in an optical dipole trap in microgravity. While one can see that the residual TDM atoms disappear radially without the gravitational force, a bright line remains in the image center, representing the optically trapped atoms.

IV. EVAPORATION

Evaporative cooling in an optical trap is carried out by a reduction of the trap depth U_0. As depicted in Fig. 5(a), the potential is tilted along the direction of gravity. This leads to an effectively lowered trap depth U_{eff} in one direction. Therefore, in the presence of gravity, evaporated atoms are preferably expelled along this direction, while there is no distinction in microgravity. An evaporation, where the possibility to leave the trap depends only on the kinetic energy in one direction ($E_g > U_0$), is called one dimensional [33]. Its efficiency is calculated to be reduced by a factor of $4\frac{U_0}{T}$ [34] in comparison to three-dimensional evaporation. The reduction can easily be understood, since atoms have to collide with each other in order to produce atoms with sufficiently high

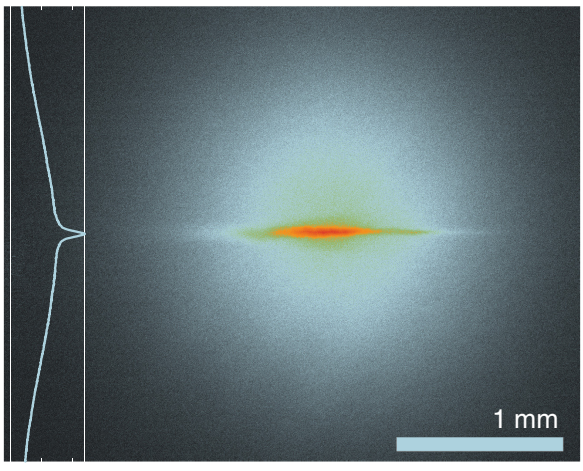

FIG. 4. False color image of the fluorescence of approximately 1 million rubidium atoms caught in an optical dipole trap in microgravity. The sharp structure in the middle represents trapped atoms while one can see nontrapped atoms disappear radially. The picture was taken 50 ms after the switching of the MOT light and magnetic field. On ground the untrapped atoms would have dropped out of the imaged area due to gravitational acceleration. The inset on the left side shows the summed fluorescent signals for every line in arbitrary units.

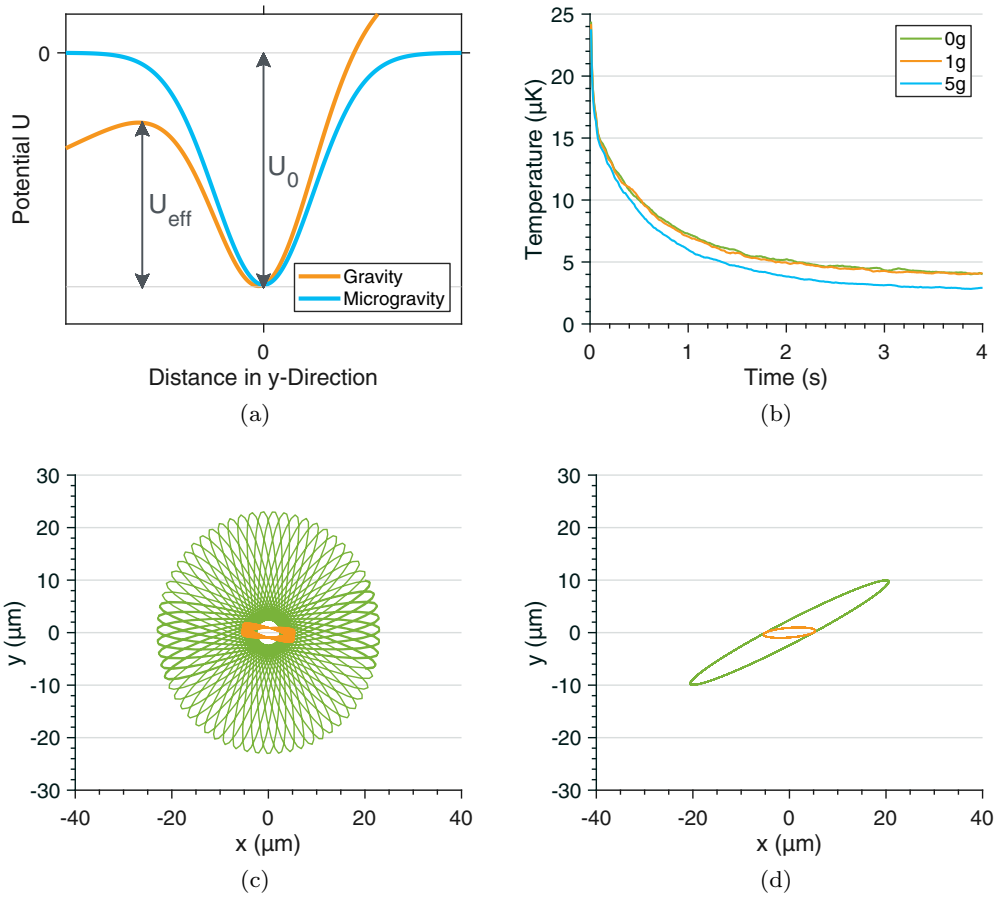

FIG. 5. (a) The optical potential along the axis of gravity is tilted, which reduces the effective trap depth in one direction. (b) DSMC simulation for an evaporative sequence for different gravitational accelerations. The temperature evolution marginally differs between the cases of microgravity (green) and ground based operation (orange). The efficiency of evaporation, and therefore the dimension of evaporation, is equal in both cases. The calculated reduction in an environment with increased gravity ($5g$) originates from a distinct reduction in trap depth and is not associated with the dimension of evaporation. (c) The trajectories of two particles in a realistic dipole trap potential with $z = 0$ (z is the trapping beam direction). The direction of kinetic energy is transferred within a few oscillations. This effect increases towards the trap edges, where the potential strongly deviates from its harmonic approximation. (d) The trajectories of two particles in a harmonic potential. The direction of kinetic energy is conserved for all velocities.

kinetic energies to leave the trap. This is the limiting process in evaporation. If the probability to leave further depends on the atomic postencounter direction, generally more collisions are needed. We simulated the process of evaporation for different values of gravitational acceleration with the DSMC (direct simulation Monte Carlo) method [35,36] and the results are shown in Fig. 5(b). The difference in temperature evolution between 1 g and 0 g is found to be marginal. Therefore the dimension of evaporation has to be (almost) similar in both cases. This result is in good agreement with the measurement from a strongly tilted trap that was published by Hung *et al.* [37]. The reason for this behavior becomes obvious by tracing the trajectories of atoms in a realistic dipole potential, as it is done in Fig. 5(c). While the direction of kinetic energy is conserved in a harmonic confining potential [Fig. 5(d)], energy can be transferred between directions in a realistic dipole potential. This is caused by the large anharmonicities at the trap edges. The figure shows two trajectories: one for an atom closer to the trap center (orange line), and a second one for an atom that reaches further out. In the second situation, that more accurately represents the case of an evaporating atom, the transfer of kinetic energy between directions is strongly increased; the potentials are mixing. In this case, the evaporation becomes three dimensional, since the initial postencounter direction does not affect the probability for an atom to be evaporated. This explanation is still in agreement with the decreased temperature evolution in the case of an increased gravitational acceleration of 5 g. Here the decisive difference is the reduction of the effective trap depth, which gets large enough to cause an observable temperature decrease. These results were confirmed with an experimental evaporative sequence in the drop tower (see Fig. 6). The dipole trap power is lowered in four linear segments with the respective final value, following $P = P_0 e^{-t/\tau} + P_f$ where P_0 is the initial laser power of 7 W (reduced by the offset), t is the time, τ represents the ramp's time constant which was chosen to be 700 ms, and P_f is the final power for an infinite time. To investigate the evaporative process, the sequence was stopped after 0.5, 1, 1.5, and 2 s respectively, followed by a free evolution time of up to 10 ms for temperature determination. We characterized the initial trap frequencies in our system to be 944 Hz in the radial and 9.2 Hz in the

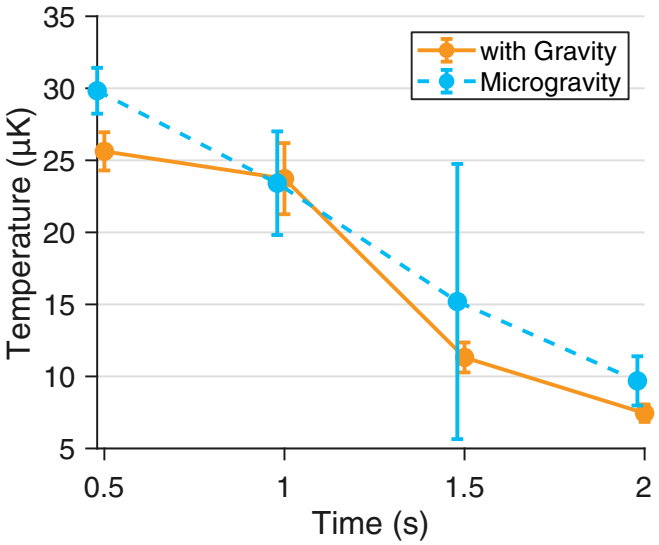

FIG. 6. Experimentally realized evaporation on ground (orange) and in microgravity (blue). Apart from the increased temperature, caused by a reduced TDM performance in microgravity, both evaporation curves are equal within the measurement uncertainties. These suffer from a limited number of underlying statistics, since at most two experiments per day, for approximately two weeks (one measurement campaign), are available.

axial direction by parametric heating and direct observation of oscillations, giving a beam waist of 45 μm for the trapping laser. This leads to a trap depth of $U_0 = k_B \times 186\ \mu$K at the beginning of our evaporation sequence. Precise temperature determinations turned out to be challenging due to the low repetition rate of two drops per day. Since it was not possible to guarantee identical starting conditions for the evaporation over the course of weeks, the recorded data suffer from a large measurement uncertainty.

V. CONCLUSION

We were able to demonstrate the loading of and evaporative cooling from an optical dipole trap in microgravity. The efficiency of evaporative cooling in weightlessness was calculated to be equal to ground based experiments. These findings were made with DSMC simulations and could be attributed to the anharmonicity of the confining potential. Furthermore, the theoretical results could be confirmed experimentally. Our results prove this kind of experiment to be feasible in a space environment as well and could lead, e.g., to improved atom interferometers, miscibility investigations, and optical lattices in microgravity on time scales of several tens of seconds. The next goal is to demonstrate the creation of an all-optical BEC which is completely prepared in microgravity. Therefore, the trapping beam will be actively pointing stabilized giving the opportunity for a crossed beam configuration with decreased evaporation times.

ACKNOWLEDGMENTS

This project was supported by the German Space Agency (DLR) with funds provided by the Federal Ministry for Economic Affairs and Energy (BMWi) due to an enactment of the German Bundestag under Grants No. DLR 50WM1642 and No. DLR 50WM1641 (PRIMUS-III). D.S. is grateful for personal funding by the Federal Ministry of Education and Research (BMBF) through the funding program Photonics Research Germany under Contract No. 13N14875.

[1] P. W. Graham, J. M. Hogan, M. A. Kasevich, S. Rajendran, and R. W. Romani, arXiv:1711.02225.
[2] B. Canuel, A. Bertoldi, L. Amand, E. Pozzo di Borgo, T. Chantrait, C. Danquigny, M. Dovale Álvarez, B. Fang, A. Freise, R. Geiger, J. Gillot, S. Henry, J. Hinderer, D. Holleville, J. Junca, G. Lefèvre, M. Merzougui, N. Mielec, T. Monfret *et al.*, Sci. Rep. **8**, 14064 (2018).
[3] D. F. Gao, J. Wang, and M. S. Zhan, Commun. Theor. Phys. **69**, 37 (2018).
[4] A. D. Cronin, J. Schmiedmayer, and D. E. Pritchard, Rev. Mod. Phys. **81**, 1051 (2009).
[5] A. Peters, K. Y. Chung, and S. Chu, Metrologia **38**, 25 (2001).
[6] V. Xu, M. Jaffe, C. D. Panda, S. L. Kristensen, L. W. Clark, and H. Müller, Science **366**, 745 (2019).
[7] J. Rudolph, N. Gaaloul, Y. Singh, H. Ahlers, W. Herr, T. A. Schulze, S. T. Seidel, C. Rode, V. Schkolnik, W. Ertmer, E. M. Rasel, H. Müntinga, T. Könemann, A. Resch, S. Herrmann, C. Lämmerzahl, T. V. Zoest, H. Dittus, A. Vogel, A. Wenzlawski *et al.*, Microgravity Sci. Technol. **23**, 287 (2011).
[8] T. van Zoest, N. Gaaloul, Y. Singh, H. Ahlers, W. Herr, S. T. Seidel, W. Ertmer, E. Rasel, M. Eckart, E. Kajari, S. Arnold, G. Nandi, W. P. Schleich, R. Walser, A. Vogel, K. Sengstock, K. Bongs, W. Lewoczko-Adamczyk, M. Schiemangk, T. Schuldt *et al.*, Science **328**, 1540 (2010).
[9] D. Becker, M. D. Lachmann, S. T. Seidel, H. Ahlers, A. N. Dinkelaker, J. Grosse, O. Hellmig, H. Müntinga, V. Schkolnik, T. Wendrich, A. Wenzlawski, B. Weps, R. Corgier, T. Franz, N. Gaaloul, W. Herr, D. Lüdtke, M. Popp, S. Amri, H. Duncker *et al.*, Nature (London) **562**, 391 (2018).
[10] B. Barrett, L. Antoni-Micollier, L. Chichet, B. Battelier, T. Lévèque, A. Landragin, and P. Bouyer, Nat. Commun. **7**, 13786 (2016).
[11] E. R. Elliott, M. C. Krutzik, J. R. Williams, R. J. Thompson, and D. C. Aveline, npj Microgravity **4**, 16 (2018).
[12] S. Stellmer, B. Pasquiou, R. Grimm, and F. Schreck, Phys. Rev. Lett. **110**, 263003 (2013).
[13] J. Hu, A. Urvoy, Z. Vendeiro, V. Crépel, W. Chen, and V. Vuletić, Science (New York, N.Y.) **358**, 1078 (2017).
[14] A. Urvoy, Z. Vendeiro, J. Ramette, A. Adiyatullin, and V. Vuletić, Phys. Rev. Lett. **122**, 203202 (2019).
[15] T. Kovachy, J. M. Hogan, A. Sugarbaker, S. M. Dickerson, C. A. Donnelly, C. Overstreet, and M. A. Kasevich, Phys. Rev. Lett. **114**, 143004 (2015).
[16] J. Rudolph, Ph.D. thesis, Institute of Quantum Optics at Leibniz University Hannover, 2016.
[17] N. Masuhara, J. M. Doyle, J. C. Sandberg, D. Kleppner, T. J. Greytak, H. F. Hess, and G. P. Kochanski, Phys. Rev. Lett. **61**, 935 (1988).

[18] H. Ammann and N. Christensen, Phys. Rev. Lett. **78**, 2088 (1997).
[19] H. Müntinga, H. Ahlers, M. Krutzik, A. Wenzlawski, S. Arnold, D. Becker, K. Bongs, H. Dittus, H. Duncker, N. Gaaloul, C. Gherasim, E. Giese, C. Grzeschik, T. W. Hänsch, O. Hellmig, W. Herr, S. Herrmann, E. Kajari, S. Kleinert, C. Lämmerzahl *et al.*, Phys. Rev. Lett. **110**, 093602 (2013).
[20] J. Reichel, W. Hänsel, and T. W. Hänsch, Phys. Rev. Lett. **83**, 3398 (1999).
[21] M. Keil, O. Amit, S. Zhou, D. Groswasser, Y. Japha, and R. Folman, J. Mod. Opt. **63**, 1840 (2016).
[22] G. Condon, M. Rabault, B. Barrett, L. Chichet, R. Arguel, H. Eneriz-Imaz, D. Naik, A. Bertoldi, B. Battelier, P. Bouyer, and A. Landragin, Phys. Rev. Lett. **123**, 240402 (2019).
[23] D. Aguilera, H. Ahlers, B. Battelier, A. Bawamia, A. Bertoldi, R. Bondarescu, K. Bongs, P. Bouyer, C. Braxmaier, L. Cacciapuoti, C. Chaloner, M. Chwalla, W. Ertmer, M. Franz, N. Gaaloul, M. Gehler, D. Gerardi, L. Gesa, N. Gürlebeck, J. Hartwig *et al.*, Class. Quantum Grav. **31**, 159502 (2014).
[24] Y. A. El-Neaj, C. Alpigiani, S. Amairi-Pyka, H. Araujo, A. Balaz, A. Bassi, L. Bathe-Peters, B. Battelier, A. Belic, E. Bentine, J. Bernabeu, A. Bertoldi, R. Bingham, D. Blas, V. Bolpasi, K. Bongs, S. Bose, P. Bouyer, T. Bowcock, W. Bowden *et al.*, arXiv:1908.00802.
[25] S. Kulas, C. Vogt, A. Resch, J. Hartwig, S. Ganske, J. Matthias, D. Schlippert, T. Wendrich, W. Ertmer, E. Maria Rasel, M. Damjanic, P. Weßels, A. Kohfeldt, E. Luvsandamdin, M. Schiemangk, C. Grzeschik, M. Krutzik, A. Wicht, A. Peters, S. Herrmann, and C. Lämmerzahl, Micrograv. Sci. Technol. **29**, 37 (2017).
[26] C. Vogt, Ph.D. thesis, University of Bremen, 2019.
[27] J. Schoser, A. Batär, R. Löw, V. Schweikhard, A. Grabowski, Y. B. Ovchinnikov, and T. Pfau, Phys. Rev. A **66**, 023410 (2002).
[28] M. Zaiser, J. Hartwig, D. Schlippert, U. Velte, N. Winter, V. Lebedev, W. Ertmer, and E. M. Rasel, Phys. Rev. A **83**, 035601 (2011).
[29] S. Rosi, A. Burchianti, S. Conclave, D. S. Naik, G. Roati, C. Fort, and F. Minardi, Sci. Rep. **8**, 1301 (2018).
[30] R. Grimm, M. Weidemüller, and Y. B. Ovchinnikov, Adv. At. Mol. Opt. Phys. **42**, 95 (2000).
[31] R. Cornelussen, Ph.D. thesis, University of Amsterdam, 2004.
[32] S. J. M. Kuppens, K. L. Corwin, K. W. Miller, T. E. Chupp, and C. E. Wieman, Phys. Rev. A **62**, 013406 (2000).
[33] W. Ketterle and N. J. V. Druten, Adv. Atom. Mol. Opt. Phy. **37**, 181 (1996).
[34] E. L. Surkov, J. T. M. Walraven, and G. V. Shlyapnikov, Phys. Rev. A **53**, 3403 (1996).
[35] G. Bird, *Molecular Gas Dynamics and the Direct Simulation of Gas Flows*, 2nd ed. (Clarendon, Oxford, 1994).
[36] H. Wu and C. J. Foot, J. Phys. B **29**, L321 (1996).
[37] C. L. Hung, X. Zhang, N. Gemelke, and C. Chin, Phys. Rev. A **78**, 011604(R) (2008).